Analysis of Protein and Peptide Penetration into Membranes by Depth-Dependent Fluorescence Quenching: Theoretical Considerations

Alexey S. Ladokhin
Department of Physiology and Biophysics, University of California-Irvine, Irvine, California 92697-4560 USA

ABSTRACT Depth-dependent fluorescence quenching in membranes is playing an increasingly important role in the determination of the low resolution structure of membrane proteins. This paper presents a graphical way of visualizing membrane quenching caused by lipid-attached bromines or spin labels with the help of a depth-dependent fluorescence quenching profile. Two methods are presently available to extract information on membrane penetration from quenching: the parallax method (PM; Chattopadhyay, A., and E. London, 1987. *Biochemistry*. 26:39–45) and distribution analysis (DA; A. S. Ladokhin, 1993. *Biophys. J.* 64:290*a* (Abstr.); A. S. Ladokhin, 1997. *Methods Enzymol.* 278:462–473). Analysis of various experimental and simulated data by these two methods is presented. The effects of uncertainty in the local concentration of quenching lipids (due to protein shielding or nonideality in lipid mixing), the existence of multiple conformations of membrane-bound protein, incomplete binding, and uncertainty in the fluorescence in nonquenching lipid are described. Regardless of the analytical form of the quenching profile (Gaussian function for DA or truncated parabola for PM), it has three primary characteristics: position on the depth scale, area, and width. The most important result, not surprisingly, is that one needs three fitting parameters to describe the quenching. This will keep the measures of the quenching profile independent of each other resulting in the reduction of systematic errors in depth determination. This can be achieved by using either DA or a suggested modification of the PM that introduces a third parameter related to quenching efficiency. Because DA utilizes a smooth fitting function, it offers an advantage for the analysis of deeply penetrating probes, where the effects of transleaflet quenching should be considered.

INTRODUCTION

Determination of membrane organization and dynamics is one of the most challenging problems in structural biology. An important aspect involves characterization of the transverse location of proteins and peptides in the bilayer (White and Wiener, 1995; Hubbell and Altenbach, 1994; White and Wimley, 1994). The depth-dependent fluorescence quenching technique, utilizing lipids with bromine atoms or spin labels selectively attached to certain positions along their acyl chains, is a useful tool to explore the membrane structure along the depth coordinate (Everett et al., 1986; Berkhout et al., 1987; Voges et al., 1987; Bolen and Holloway, 1990; Clague et al., 1991; Yeager and Feigenson, 1990; Meers, 1990; Chung et al., 1992; González-Mañas et al., 1992; Ladokhin et al., 1993a, b; Matsuzaki et al., 1994; Jones and Gierasch, 1994; Ladokhin and Holloway, 1995a, b; Sassaroli et al., 1995; Asuncion-Punzalan and London, 1995; Kachel et al., 1995; Castanho and Prieto, 1995; Macêdo et al., 1996; Mishra and Palgunachari, 1996; Oren and Shai, 1997; Liu and Deber, 1997). The PM (Chattopadhyay and London, 1987; Abrams and London, 1992, 1993) and DA (Ladokhin, 1993, 1997) can be utilized to quantitate this quenching in order to extract information on membrane penetration. Previously we have compared the quality of fit provided by these two methods and discussed their underlying physical assumptions (Ladokhin and Holloway, 1995a; Ladokhin, 1997). We have demonstrated that application of DA, which has three fitting parameters (compared to two for PM), is not only statistically justifiable but, more importantly, yields additional valuable information on the fluorophore's transverse heterogeneity and lipid exposure. This report presents an evaluation of the capabilities of the two methods, based on their treatment of various experimental and simulated data. Specifically, the systematic errors that affect determinations of the depth of the fluorophore are analyzed with respect to the number of the free fitting parameters employed to describe quenching.

This paper presents a graphical way of visualizing membrane quenching with the help of a depth-dependent fluorescence quenching profile. Regardless of its analytical form, the quenching profile has three primary characteristics: position on the depth scale, area, and width. Quenching profiles provided by DA and the PM are examined with respect to how they are affected by uncertainty in the local

Received for publication 25 June 1998 and in final form 22 October 1998.

Address reprint requests to Dr. Alexey S. Ladokhin, Department of Physiology and Biophysics, University of California-Irvine, 346-D Med. Sci. I, Irvine, CA 92697-4560. Tel.: 949-824-6993; Fax: 949-824-8540; E-mail: ladokhin@uci.edu.

Permanent address: Institute of Molecular Biology and Genetics, National Academy of Sciences of Ukraine, Kiev 252143, Ukraine.

Abbreviations used: PM, parallax method; DA, distribution analysis; LUV, large unilamellar vesicles of 100 nm diameter, obtained by extrusion; MSP, the membrane spanning peptide of Bolen and Holloway (1990); OmpA, outer membrane protein A; 4-5, 6-7, 9-10, 11-12, or 15–16BPC, 1-palmitoyl2(dibromostearoyl)phosphatidylcholine with bromine atoms at the 4-5, 6-7, 9-10, 11-12, or 15-16 positions, respectively; POPC, palmitoyloleoylphosphatidylcholine; quenching profile or profile, depth-dependent fluorescence quenching profile; SUV, small unilamellar vesicles of 30 nm diameter, obtained by sonication; TOE, tryptophan octyl ester.

0006-3495/99/02/946/10 $2.00

concentration of quenching lipids (due to protein shielding or nonideality in lipid mixing), the existence of multiple conformations of membrane-bound protein, incomplete binding, and uncertainty in the fluorescence in nonquenching lipid. In its present form, PM is prone to potentially significant systematic errors in the determination of depth, because area and width of the quenching profile depend on a single parameter. One can improve the performance of the PM by introducing a third independent fitting parameter, related to quenching efficiency, that uncouples the width and area. These two characteristics depend on different properties of the system (exposure to lipid and transverse heterogeneity) and therefore should be kept independent of each other during the analysis. Because DA utilizes three fitting parameters, area, width, and mean depth, its solutions are largely unaffected by any of the examined factors. Application of the DA formalism to the data of Rodionova et al. (1995) allows one to recognize large conformational change associated with membrane insertion of OmpA.

Finally, the effects of transleaflet quenching are addressed, applying a new procedure that accounts for the phenomenon by adding to the original profile a symmetrical component on the *trans* side of the bilayer (Ladokhin, 1997). Because DA, unlike PM, operates with a smooth fitting function, this modification is easy to implement. I analyzed data published by Bolen and Holloway (1990) on a synthetic membrane spanning peptide designed to adopt an α-helical transmembrane conformation and to bring its single tryptophan close to the center of the bilayer. This analysis demonstrates that DA can be used to evaluate a wide range of membrane penetrations.

THEORY

In a depth-dependent fluorescence quenching experiment one determines the fluorescence intensity, F, of a probe as a function of the known depth of the quencher, h. Data are usually normalized to the intensity in the absence of quenching, F_0. Two methods, PM (Chattopadhyay and London, 1987) and DA (Ladokhin, 1993, 1997) are used to quantitate the quenching. The principal equations for these methods, rewritten in a similar form for ease of comparison, are:

$$\text{DA:}\quad \ln\frac{F_0}{F(h)}\cdot c(h) = \frac{S}{\sigma\sqrt{2\pi}}\cdot\exp\left[-\frac{(h-h_m)^2}{2\sigma^2}\right] \tag{1}$$

$$\text{PM:}\quad \ln\frac{F_0}{F(h)}\cdot c(h) = \pi\cdot C\cdot[R_c^2-(h-h_m)^2],\quad h-h_m < R_c \tag{2}$$

$$\ln\frac{F_0}{F(h)}\cdot c(h) = 0,\quad h-h_m \geq R_c$$

The identical left-hand side is a function of the fluorescence corrected for the difference in concentration of different quenchers, $c(h)$. For simplicity of presentation only, we will consider the case when concentrations of different quenchers are equal to each other, so that $c(h) = 1$. The expression on the left-hand side will be called the depth-dependent fluorescence quenching profile.

On the right are analytical expressions for the quenching profile represented by either a Gaussian function (DA) or truncated parabola (PM). Examples of quenching profiles

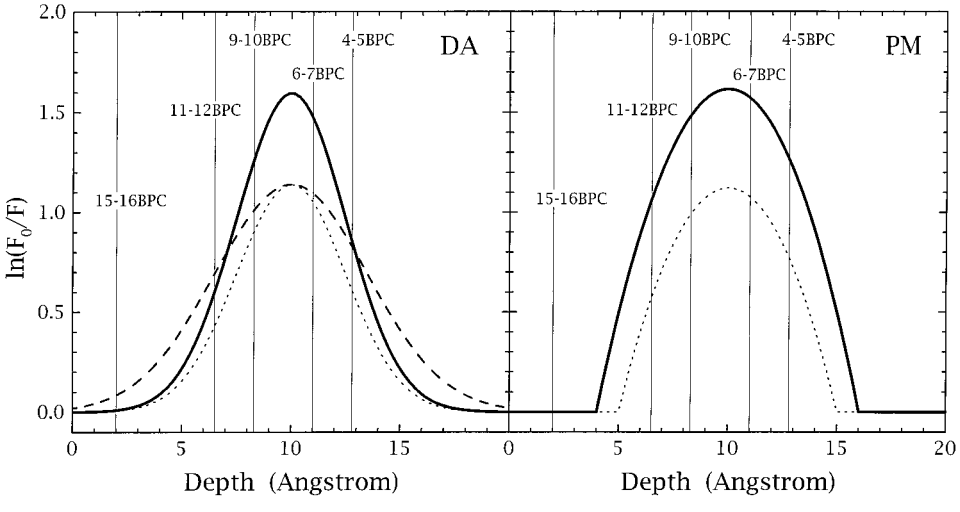

FIGURE 1 Depth-dependent fluorescence quenching profiles are used to visualize the change in fluorescence, F, of a probe (normalized to its value in the absence of quenching, F_0) when the quencher is present at a certain depth in the bilayer. The depth scale is defined in such a way that zero is placed in the middle of the bilayer. Distribution analysis (DA) and the parallax method (PM) describe the quenching profile as a Gaussian (Eq. 1) and truncated parabola (Eq. 2), respectively. Vertical lines are drawn at the depth positions where quenching can be experimentally probed with the indicated brominated lipids. Because DA operates with three parameters, it allows the area and width of the profile to be changed independently (*dotted* and *dashed lines*). The PM uses only two parameters, therefore the changes in area and width are coupled (*dashed line*). Unlike that of the PM, the quenching profile for DA is a smooth function.

are presented in Fig. 1. The Gaussian function has the following three parameters: mean depth (h_m), dispersion (σ), and area (S). Note that PM operates on only two fitting parameters: mean depth (h_m), and radius of quenching (R_c), and that the area and width of the profile are coupled to a single parameter, R_c, and cannot be changed independently (Fig. 1). The third parameter, C, is the known quencher concentration and does not vary in the analysis. It is usually expressed as the surface concentration.

Traditionally, PM is used as an analytical procedure to calculate depth and R_c, from two measurements of intensity, using an equation derived from Eq. 2 (Chattopadhyay and London, 1987). Here the principal equation (Eq. 2) is used predominantly, because it allows the fitting of multiple data points and facilitates visualization of the quenching profile.

METHODS

Most of the simulations presented here are based on data for the quenching of TOE with bromolipids (Ladokhin et al., 1993a). The depth of bromines was estimated from the x-ray diffraction data of McIntosh and Holloway (1987). When the effects of incomplete binding and variations of F_0 were analyzed, the number of data points was reduced to achieve zero degrees of freedom for both the DA and PM fits. This was done to eliminate uncertainties associated with random errors caused by data scattering and to focus on systematic errors in determination of depth. Fluorescence measured with lipids brominated at the following positions along the *sn*-2 acyl chain was used: 4-5; 9-10; 11-12 for DA, and 4-5; 11-12 for PM. Therefore, the recovered parameters are slightly different from those previously reported, in which data for all four quenchers were utilized in the fit (Ladokhin and Holloway, 1995a). The overall conclusions, however, do not depend on the selection of quenchers. We used a value of 70 Å^2 for area for one lipid molecule (Lewis and Engelman, 1983) to express C in the PM. Variation in degree of binding was simulated by adding the desired contributions of bound and free probe multiplied by the corresponding quantum yields. Variation in F_0 was simulated by multiplying the intensity measured in POPC by a factor of 2 or 0.5. Further details are described in the Results section. Data analysis using a least-squares minimization routine and graphic representation of results were performed with the commercial software package Origin 3.5 (MicroCal, Inc., Northampton, MA).

RESULTS

The basic approach taken in the subsequent analysis consists of the following three steps: 1) assume that the quenching profile is indeed a Gaussian function (for DA) or a truncated parabola (for PM); 2) introduce a certain variation in physical property (protein shielding, multiple conformations, incomplete binding, etc.); 3) evaluate the quality of data description and estimate possible systematic errors introduced by this variation.

Variation in the local concentration of quenchers

The concentration of quenching lipids in the vicinity of the fluorophore could be quite different from that in the bulk of the membrane. Effects of the variation in this local concentration of quenchers on solutions provided by DA and PM are presented in Fig. 2. Squares correspond to quenching of the TOE fluorescence with a set of four bromolipids (Ladokhin et al., 1993a). The local concentration of quenchers, C_f, is expressed as a variable fraction, f, of the total concentration of quenchers, C, such that $C_f = f \cdot C$. Systematic changes in f from 0.1 to 1 are made in increments of 0.1, and the effects on the fit of the TOE data (*lines* in Fig. 2) are considered. Because DA does not explicitly depend on the quencher concentration C (Eq. 1), its solutions are unaffected by variation in f (Fig. 1, *left*). All curves have the following parameters: $h_m = 11.3$ Å; $S = 18.9$; $\sigma = 5.5$ Å.

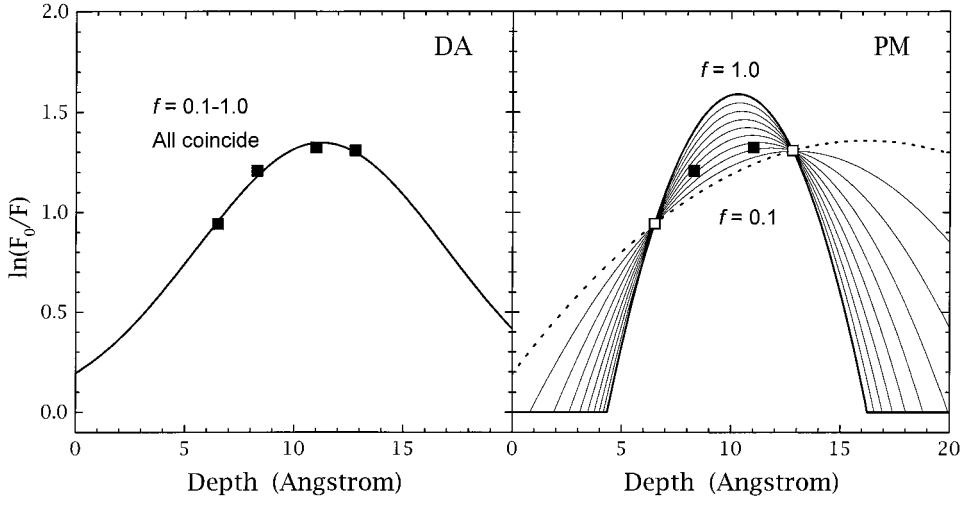

FIGURE 2 Effects of variation in the fraction of quenching lipids in the vicinity of the fluorophore on solutions provided by DA and PM. Squares correspond to quenching of TOE fluorescence with the set of bromolipids (Ladokhin et al., 1993a). Local concentration of quenchers is expressed as a fraction, f, of the total concentration of quenchers. Because DA does not explicitly utilize the value for the concentration of quenchers (Eq. 1), its solutions are not affected by changes in f (*left panel*). Solutions provided by the PM (Eq. 2), however, show significant variation with changes of f (*right panel*), introducing a potentially significant systematic error in the determination of depth (see text for details). The best description of the data is achieved for the intermediate level of $f = 0.3$–0.4 but not for $f = 1$, as assumed by the original PM.

Unlike DA, the PM relies on explicit knowledge of C (Eq. 2). Therefore its solutions will vary with changes in f. Following the analytical PM procedure (Chattopadhyay and London, 1987) two points from the TOE data set (*open squares*) are used to recover two parameters, h_m and R_c. These parameters are then used to recreate the complete quenching profile, with Eq. 2 substituting $C_f = f \cdot C$ for C. For a clearer graphical presentation two limiting data points are used. The overall results were the same whether any other pair of points was used or all four points were used, and curves were fitted by a least-squares procedure.

As expected, solutions provided by the PM show a significant variation with changes of f (Fig. 2, *right*). This is likely to introduce a potentially significant systematic error in the determination of depth, because the standard PM procedure assumes $f = 1$ (*thick line*). If, for example, the real f were equal to 0.1 (*dotted line*), the difference between the actual depth of the probe and the solution provided by the PM would be as big as 6 Å (the difference between maxima of *thick solid* and *dotted curves* in Fig. 2, *right*). Because the fraction of quenchers interacting with the fluorophore is not known, it is reasonable to use it as a third free parameter. This, in turn, will require a third data point on the depth scale. When the remaining points (*solid squares*, Fig. 2, *right*) are added, it becomes clear that the best description of the entire data set is achieved for the intermediate level of $f = 0.3–0.4$. When f is used as a free fitting parameter (curve not shown) the following parameters are recovered: $h_m = 11.4$ Å; $f = 0.38$; $R_c = 8.9$ Å. Note that the value for the mean position now practically coincides with that predicted by DA.

This also means that at this point, the exact functional form of the quenching profile is not nearly as important as the number of independent parameters. Indeed, a Gaussian function and a three-parameter parabola have the same ability to describe the data. Obviously the Gaussian is a more physically relevant function to describe transverse distribution of membrane moieties, which follows from general considerations of the central limit theorem and direct confirmation by diffraction experiments of Wiener and White (1991). Additional advantages of the Gaussian function for quenching studies will become apparent in further analysis (see Transleaflet Quenching).

It has been noted that the PM results vary with the pair of quenchers used and it has been suggested that only the two strongest quenchers be used in the analysis (Abrams and London, 1992, 1993). We find no need for any restriction on the data provided a third parameter is introduced (see also Example of Conformational Change Monitored by Membrane Quenching). Certainly, if the two best quenchers were used in the PM analysis of the TOE data in Fig. 2, the variation in h_m with the changes in f will be reduced. This is hardly surprising in this particular case, because the two strongest quenchers produce almost identical quenching, and their depth is separated by only 1.8 Å. Nevertheless, the optimal description of all data was achieved for $f = 0.3–0.4$ regardless of the pair of quenchers used.

Multiple conformations of membrane-bound protein

Effects of the conformational heterogeneity of fluorophore/peptide on solutions provided by DA and the PM are presented in Fig. 3. The simplest case was considered: a hypothetical peptide with two populations, one shallow (*thin*

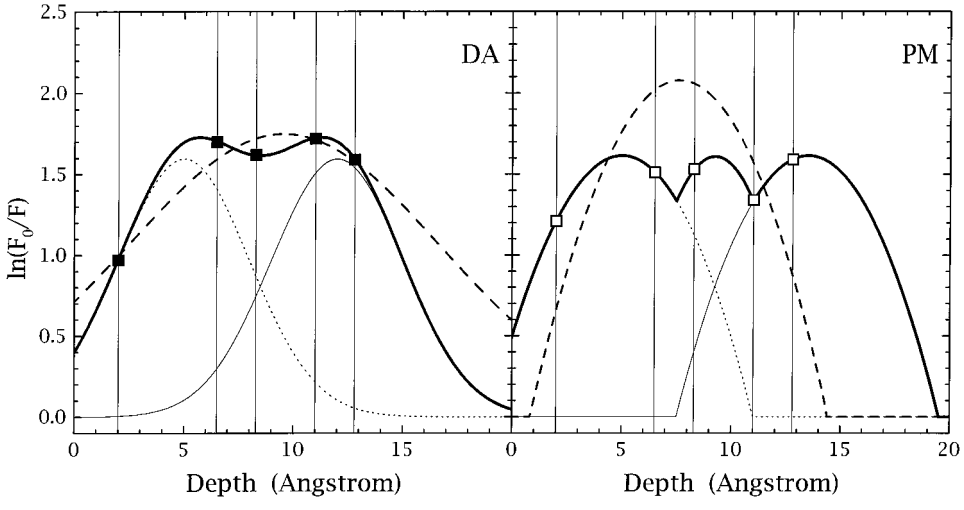

FIGURE 3 Effects of the conformational heterogeneity of fluorophore/peptide on solutions provided by DA and the PM. Two moderately resolved populations (separation equal to the width of the quenching profile) with shallow (*thin solid lines*) and deep (*dotted lines*) mean depth were simulated by either Gaussian (*left panel*) or truncated parabola (*right panel*). The sum of the two (*thick line*) is the total profile that can be probed experimentally at points represented by squares (see also legend to Fig. 1). Dashed lines correspond to unimodal DA (Eq. 1) and the PM (Eq. 2) best fit approximations of the simulated data sets (*squares*). DA not only results in a much better fit, but also recovers a solution with large width, indicative of conformational heterogeneity.

solid lines) and one deep (*dotted lines*), but with otherwise identical quenching profiles. These two populations, modeled by Gaussians (DA) or truncated parabolas (PM), were located in the bilayer with a separation in depth equal to the width of the profile. The sum of the two (*thick line*) is the total quenching profile that can be probed experimentally at points represented by squares. A set of five bromolipids was used as an example of the maximal number of quenchers used in a single experiment (Bolen and Holloway, 1990), but even this number is not sufficient to resolve the two populations in a general case. Instead, the simulated five points will be fit with a single unimodal distribution for each method (*dashed lines*), to ascertain whether the parameters obtained indicate the possibility of multiple conformations. Indeed, DA recovers a distribution with such a large width that the quenching profile seems to be occupying space significantly larger than the dimensions of the bilayer. This artificially large width is indicative of conformational heterogeneity. Previously, such behavior was reported for a bee venom peptide, melittin, suggesting the possibility of multiple conformations of peptide in the bilayer (Ladokhin and Holloway, 1995b).

Note that the DA fit to simulated data is rather good (Fig. 3, *left*). However, application of the PM results in a poor fit (Fig. 3, *right*), and the recovered width is exactly the same as for the individual subpopulation. Thus, the PM in its present form does not give any indication of the possibility of multiple conformations. The quality of the fit can be improved by introducing a third fitting parameter, *f*, discussed above (curve not shown). The resulting profile will have a large width, consistent with imputed heterogeneity.

Incomplete binding and uncertainty in F_0

The results of DA and PM evaluation of data simulating incomplete binding are shown in Table 1. The simulation is based on the experimentally obtained quenching of the TOE (Ladokhin et al., 1993a; Ladokhin and Holloway, 1995a) and was performed utilizing reduced data sets as described in Methods. Data simulated for 75%, 50%, and 25% binding were fitted by Eq. 1 or Eq. 2, under an implicit assumption of complete binding. The resulting parameters are to be compared to those for 100% binding.

The variation in binding, evaluated by DA, has a strong effect only on the area under the quenching profile. This is not surprising because the overall quenching is reduced since the fluorescence of the molecules not bound to the membrane cannot be quenched. However, the quantum yield of bound and unbound molecules is different even without the depth-dependent quenching. Therefore the relative change in *S* differs from the relative change in binding. The width of the profile is somewhat sensitive to the binding, but the maximal change in σ of 20% should be considered to be moderate. Most importantly, the solutions are very robust with regard to the mean depth, h_m. Thus, if in a real experiment the fraction of bound peptide is not known, DA will still provide a correct answer for the depth.

Under the same conditions, both parameters recovered with the PM undergo a continuous shift (Table 1). Though noticeable in the simulations, the maximal change of 0.5 Å in mean depth should be considered tolerable in evaluations of most experimentally measured data.

The tactics described above were applied to the evaluation of the effects of the variation in fluorescence in all nonquenching lipid, F_0. F_0 was altered for the same data set for TOE (Ladokhin et al., 1993a) by a factor of 2 or 0.5, and the recovered parameters were compared with those for the true F_0 (Table 2). This is shown to have a marginal (DA) or zero effect (PM) on the determination of depth, while significantly altering the other parameters.

Example of conformational change monitored by membrane quenching

The difference in the information provided by DA and the PM is shown in the analysis of the bilayer penetration of the OmpA, for which fluorescence quenching with a set of three bromolipids in the DMPC matrix has recently been reported (Rodionova et al., 1995). OmpA makes a convenient test case because of the proposed existence of two forms depending on the state of the lipid.

The data for OmpA quenching at 4°C (*solid squares*) and at 30°C (*open squares*) are presented in Fig. 4. The best fit approximations using DA (Eq. 1, *solid lines, panel A*) and PM (Eq. 2, *dotted lines, panel A*) indicate a temperature

TABLE 1 Effects of the simulated incomplete binding of TOE on solutions provided by DA and PM

Probe/peptide bound to membrane	DA			PM	
	h_m (Å);	*S*;	σ (Å)	h_m (Å);	R_c (Å)
100%	11.0;	18.0;	5.2	10.3;	6.0
75%	11.0;	14.9;	5.5	10.1;	5.5
50%	11.0;	11.3;	5.8	9.9;	5.0
25%	11.0;	6.6;	6.3	9.8;	4.2

See text for details. For DA the changes are limited to *S* and σ, while for PM both parameters are altered. Therefore, if in a real experiment the fraction of bound peptide is not known, DA will still provide a correct answer for the depth.

TABLE 2 Effects of the simulated variation of fluorescence of TOE in nonquenching lipid on solutions provided by DA and PM

True fluorescence with no quenching	DA			PM	
	h_m (Å);	*S*;	σ (Å)	h_m (Å);	R_c (Å)
F_0*	11.0;	18.0;	5.2	10.3;	6.0
$2 \cdot F_0$*	11.1;	34.6;	6.7	10.3;	7.1
$0.5 \cdot F_0$*	10.9;	5.6;	3.0	10.3;	4.5

See text for details. Two-fold changes in F_0 have marginal (DA) or zero effect (PM) on the determination of depth, while significantly altering the other parameters.

*Fluorescence in POPC (Ladokhin and Holloway, 1995a).

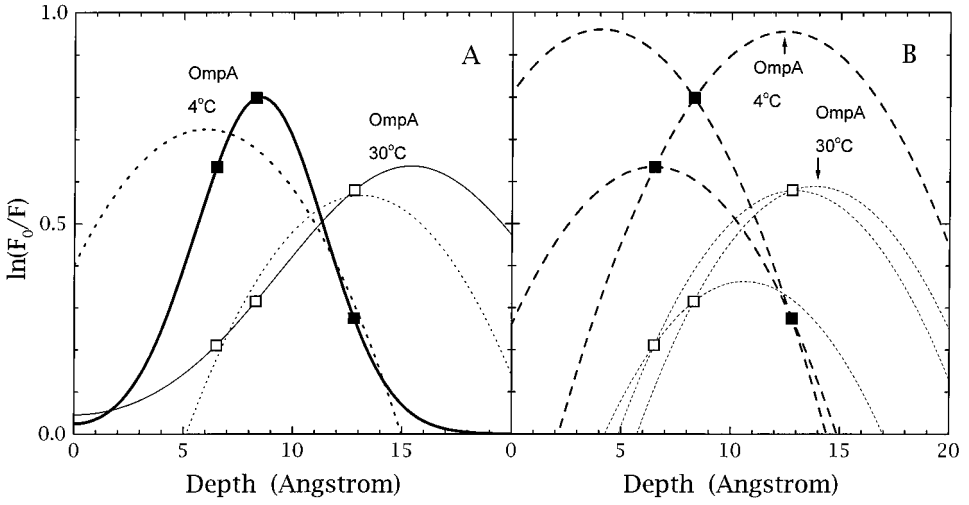

FIGURE 4 Analysis of depth-dependent fluorescence quenching of OmpA with DA and the PM. Data for 4°C (*solid squares*) and 30°C (*open squares*) were obtained using 20% bromolipid vesicles (Rodionova et al., 1995). Application of DA results in quenching profiles for the two temperatures (*solid curves, panel A*) that differ not only in position, but in width and area as well (see text). Best fit PM approximations (*dotted lines, panel A*) indicate the change in position but have similar R_c parameters (see text). A pairwise analysis of quenching with the original PM (*dashed lines, panel B*) produces results that are subject to large variations depending on the pair of quenchers used. Arrows indicate solutions obtained with the pairs of strongest quenchers. Only the DA results suggest that temperature change causes a substantial conformational change, which alters exposure of tryptophan residues to the lipid quenchers.

controlled change in insertion. The following parameters are recovered:

$$\text{DA:}\quad \begin{array}{llll} h_m = 8.5\ \text{Å} & S = 5.9 & \sigma = 2.9\ \text{Å} & \text{at } 4°\text{C} \\ h_m = 15.4\ \text{Å} & S = 9.5 & \sigma = 6.0\ \text{Å} & \text{at } 30°\text{C} \end{array}$$

$$\text{PM:}\quad \begin{array}{lll} h_m = 6.0\ \text{Å} & R_c = 9.0\ \text{Å} & \text{at } 4°\text{C} \\ h_m = 13.1\ \text{Å} & R_c = 8.0\ \text{Å} & \text{at } 30°\text{C} \end{array}$$

In this case both methods give similar depth results and suggest a deeper average location of quenchable tryptophans at the lower temperature. The DA, however, provides additional information that indicates that the quenching profiles for OmpA at these two temperatures differ dramatically both in width and area. This suggests a massive conformational change that alters exposure of tryptophan residues to the lipid phase. Part of this change could also arise from the possible phase separation of brominated and nonbrominated lipids, which might affect quenching at lower temperatures. However, the PM, which couples both area and width to a single parameter R_c, gives no indication of such a change.

Fig. 4 *B* contains the same data for OmpA as well as the quenching profiles reconstructed from a pairwise analysis of quenching (*dashed lines*) according to the original analytical PM procedure (Chattopadhyay and London, 1987). The results produced are subject to a large variation, depending on the pair of quenchers used, which can obscure meaningful interpretation. Even choosing the pair with the strongest quenching could produce a misleading result (these solutions are marked with arrows). To avoid such pitfalls it is necessary to use all experimentally available data in a minimization procedure.

Transleaflet quenching

For simplicity of presentation, the possibility of additional quenching coming from groups located in the sides of the bilayer opposite the probe has been ignored in the analysis above. Because of the great thermal disorder, demonstrated by both experimental and computational methods (White and Wiener, 1995; Pastor et al., 1991) these effects cannot be neglected, especially when the probe is located deep in the membrane. Recently a procedure was suggested that accounts for the phenomenon by adding to the original quenching profile of a symmetrical component on the *trans* side of the bilayer (Ladokhin, 1997).

This procedure is illustrated by simulations of the quenching profile of a hypothetical probe in Fig. 5. The thick solid line represents the profile for quenching coming from a *cis* side of the bilayer (probe and quencher belong to the same leaflet). The dotted line represents the profile for *trans* side quenching (probe and quencher belong to the opposite leaflets) and is a mirror image of the former. Because in the typical experiment quenchers are distributed in both leaflets, a quencher is always located across the bilayer from a probe, regardless of whether the probe occupies two leaflets or one. Therefore, the total quenching profile is the sum of two symmetrical components (*light solid line*).

Unless some specific procedure is used to introduce the asymmetry of quenchers (Everett et al., 1986), only the positive region of depth is experimentally accessible. As an example, in Fig. 5 vertical lines are drawn at the depth positions where quenching can be experimentally probed with a set of brominated lipids. The amount of transleaflet

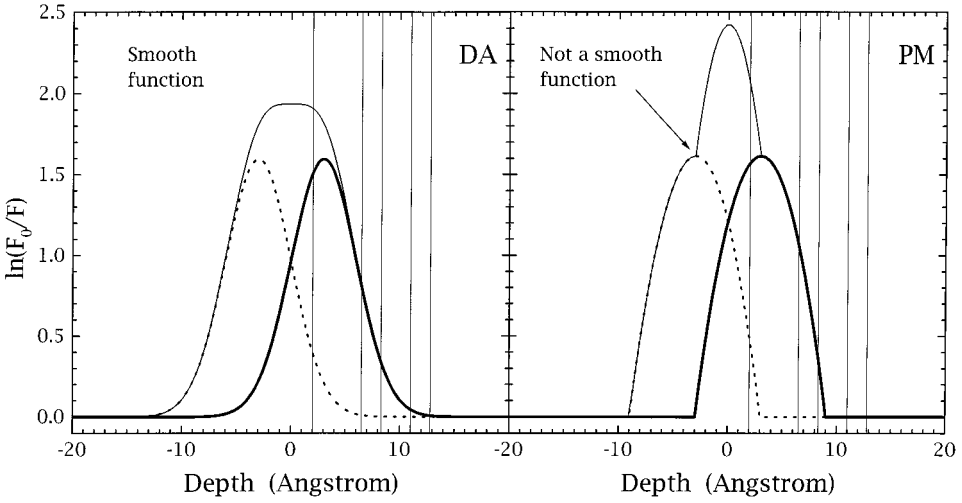

FIGURE 5 Effects of the transleaflet quenching on DA and PM quenching profiles of a hypothetical probe. The thick solid line represents the profile for quenching coming from a *cis* side of the bilayer. The dotted line represents the profile for *trans* side quenching and is a mirror image of the former. The light solid line represents a total fluorescence quenching profile. Because in the typical experiment quenchers are distributed in both leaflets, corresponding vertical lines (see legend to Fig. 1) are drawn only through the positive region of depth. Note that unlike the PM, DA results in a smooth total quenching profile, which could be easily used to fit the data (Eq. 3). This procedure utilizes the same three parameters but accounts for transbilayer quenching and allows examination of deeply penetrating fluorophores (see Fig. 6).

quenching depends on the mean position of the probe and the width of the distribution, and will be unique to each probe. Therefore there cannot be a general rule allowing for these effects to be accounted for by simple data manipulation (e.g., dividing the intensity for the deepest quencher, or its logarithm, by 2 or any other number). The transleaflet quenching also will be different for quenchers with the different depth, but not necessarily confined to the deepest one.

Because DA, unlike the PM, utilizes a smooth fitting function, the total depth-dependent fluorescence quenching profile could be easily fit to the data (Ladokhin, 1997):

$$\ln \frac{F_0}{F(h)} \cdot c(h) = G(h - h_m, S, \sigma) + G(h + h_m, S, \sigma), \qquad (3)$$

where G is a Gaussian function from the right-hand side of Eq. 1. This equation utilizes the same three parameters as Eq. 1, but accounts for transbilayer quenching and allows examination of deeply penetrating fluorophores (see Fig. 6).

The procedure is applied to examine the depth-dependent fluorescence quenching of model MSP, expected to cross the membrane in an α-helical conformation. The original data obtained by Bolen and Holloway (1990) with the set of five bromolipids are re-plotted in Fig. 6. Squares correspond to quenching in SUV, and circles to that in LUV. Solid lines in *A* correspond to the best fit error-weighted approximations, with Eq. 3 accounting for the transleaflet quenching. The following parameters are recovered (with the confidence limits estimated for the confidence probability of 0.67):

MSP in SUV:

$$h_m = 4.1 \pm 0.3 \text{ Å} \quad S = 19.8 \pm 1.1 \quad \sigma = 3.9 \pm 0.3 \text{ Å}$$

MSP in LUV:

$$h_m = 3.9 \pm 0.4 \text{ Å} \quad S = 21.5 \pm 0.7 \quad \sigma = 5.0 \pm 0.5 \text{ Å}$$

Individual quenching profiles for a single leaflet quenching are redrawn in Fig. 6 *B* for clarity of presentation. The profile for TOE in SUV (Ladokhin and Holloway, 1995a) is shown for comparison (*dotted line*). Distributions of peptide in two membrane systems appear to have the same mean position close to the center of the bilayer. The distribution in LUV is broader than that in SUV, suggesting a difference in transverse heterogeneity due, perhaps, to differences in lipid packing. In both cases the width of the distribution is smaller than that for the TOE. This indicates that the transverse freedom of peptide is restricted, perhaps by its α-helical conformation. The area under the quenching profile was found to be the same in both membrane systems. This is consistent with the expected similarity in the degree of exposure of tryptophan residue to the lipid phase.

DISCUSSION

Quantitative description of depth-dependent fluorescence quenching presents a nontrivial task, in part because of the following two reasons. First, it is a dynamic quenching for both bromolipids (Ladokhin and Holloway, 1995a, b) and spin labels (Matko et al., 1992; Clague et al., 1991; Green et al., 1990) occurring in a complex environment, where different types of motion, such as transverse fluctuations, in-plane rotation, lateral diffusion, wobbling, and density fluctuations are expected to contribute in an unknown fashion. Second, the number of data points available on the scale of depth is usually small and normally range from three to

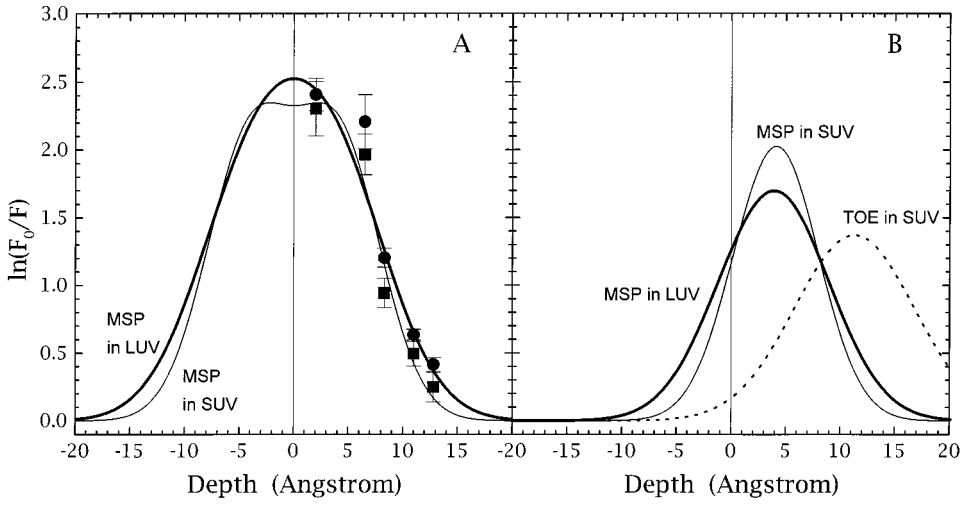

FIGURE 6 DA examination of depth-dependent quenching of fluorescence of model MSP, with the set of five bromolipids. The original data for MSP in LUV (*circles*) and SUV (*squares*) were reported by Bolen and Holloway (1990). The solid lines in *panel A* correspond to the best fit approximations, with Eq. 3 accounting for the transleaflet quenching (see parameters in text). Individual quenching profiles are shown in *panel B*. The distribution of peptide in LUV (*thick line*) appears to have the same mean position as in SUV (*thin line*), close to the center of the bilayer, but is somewhat broader. In both cases the width of the distribution is smaller than that for the model compound TOE (*dotted line*), indicating a reduction in transverse conformational freedom imposed by the helical structure. The areas under the quenching profile are similar for MSP in both systems, suggesting the same degree of exposure of tryptophan residue to lipid phase.

five, ultimately limiting the complexity of any model that can be used to describe membrane quenching.

In the recently introduced distribution analysis we use three parameters of a Gaussian function to characterize depth-dependent fluorescence quenching (Ladokhin, 1993, 1997). They are the mean position of the probe, width of the quenching profile (related to, but always larger than the width of the distribution of the probe itself), and area under the quenching profile (Eq. 1; Fig. 1, *left*). Because the PM has only two parameters, the area and the width became coupled to each other via a single parameter R_c (Eq. 2; Fig. 1, *right*). The necessity of having three parameters is proved by comparing the information provided by the two methods. Simulations are used because they allow generation of quenching profiles for systems with selectively altered properties that mimic possible variations of real systems (Figs. 2 and 3; Tables 1 and 2). All examples presented were either measured with or simulated for bromolipids. However, there is no specification of the nature of quenching group in the analysis and all of the conclusions equally apply to quenching with spin labels.

Of course, any method describing depth-dependent quenching relies on knowledge of quencher depth. Although this depth is usually known (or assumed to be known) for quencher in a pure lipid environment, it might be altered by the presence of peptide. However, these alterations can neither be measured accurately nor modeled with any reasonable confidence. Moreover, because these effects are expected to be different for different peptides, no generalized prediction could be attempted. Therefore, the errors introduced by uncertainty in the depth position of quencher were not considered in this paper.

The most profound result is the effect of the variation of quencher concentrations on the quenching profile (Fig. 2). When conducting the quenching experiment in membranes, the overall concentration of quenchers, C, is known and can be manipulated. However, the concentration of quenchers in the fluorophore's environment that actually produces quenching, C_f, is never known. There are several possible sources for the difference between C and C_f. It can be caused by a nonideality of mixing quenching and nonquenching lipid or direct interaction of peptide with the quenching lipid. These are the kind of effects that should be explored by careful measurements of concentration dependence of quenching, and are considered to be rare (Silvius, 1992; Piknová et al., 1996).

A second and much more general source of uncertainty in C_f includes the effects of protein shielding. Tryptophan residues in different proteins could be located at identical depth, but have different exposure to the lipid phase. Because quenching with bromine atoms or spin labels is a short-range one [(Berlman, 1973; Green et al., 1990) and discussion below], variation in exposure will affect the amount of quenching. This certainly will be different for a long-range quenching, such as a Förster dipole-dipole energy transfer.

All PM equations (Chattopadhyay and London, 1987; Abrams and London, 1992, 1993) assume, by default, that $C = C_f$. (From now on these methods will be referred to as "original PM.") However, when a third fitting parameter, f, is formally introduced as $f = C/C_f$, the PM describes the data more adequately (Fig. 2, *right*). In mathematical terms this third parameter allows an uncoupling of the area and the width of the quenching profile, so they can be changed

independently (Area = $4.19 \cdot C \cdot f \cdot R_c^3$; Full Width = $1.41 \cdot R_c$). In DA, the area and the width are already independent and are conveniently represented by two individual parameters (Area = S; Full Width = $2.35 \cdot \sigma$). These parameters are related to the quenchability of the fluorophore and its transverse heterogeneity, respectively (Ladokhin and Holloway, 1995a; Ladokhin, 1997). The solutions provided by DA for the certain data set are independent of the assumptions on the concentration of quenchers in the vicinity of a probe (Fig. 2, *left*). However, this does not mean that DA ignores possible differences in exposure of tryptophan residues to the lipid phase. On the contrary, the area parameter S provides the means to quantitate this exposure as a fraction of that for a model tryptophan-containing compound. This extended DA procedure is described in detail elsewhere (Ladokhin, 1997).

The variation in quenching efficiency caused by acyl chain packing differences in different membranes or by nonideal mixing of fluorophore and quencher will have the same effect as protein shielding on the determination of depth. Using three fitting parameters, one would be able to minimize systematic errors in determination of depth. In the case of DA these variations will only affect the S parameter, since area and width are uncoupled.

The same feature of DA, namely independence of area and width of the quenching profile, is important for the analysis of transverse heterogeneity (Fig. 2). The simulation reported here used the simplest case of a peptide with two distinct conformations in the membrane. In reality, several phenomena can result in heterogeneity of penetration; also, the inherent width of the transverse distribution for different peptides could be different, even though they might have a unique population in the membrane. The width of the quenching profile will also depend on the physical size of the fluorophore and quencher. A way to estimate the width of the distribution of the fluorophore itself from the width of the quenching profile has been recently described (Ladokhin, 1997) using certain simplifying assumptions and additional information on diffraction of the quenchers (Wiener and White, 1991). If this information is not readily available, the estimates could be done by comparing the width of the quenching profile for the studied peptide to that for the model compound, such as TOE (Fig. 6).

The challenging real system example for the quenching analysis is presented by the membrane-bound OmpA that, depending on the state of the lipid, can be found in two forms (Rodionova et al., 1995). These two forms have different effective average depths of penetration of tryptophans, which are detected by both methods (Fig. 4). DA detects that the deeper insertion is accompanied by substantial rearrangement, resulting in a different exposure of tryptophans to the lipid quenchers, when PM does not. The molecular details of this rearrangement are currently being addressed by Kleinschmidt and Tamm (1998) with the help of single tryptophan-containing mutants.

An advantage of using a smooth fitting function, as in DA (Eq. 1; Fig. 1), becomes important when analyzing the quenching of deeply penetrating fluorophores. In this case the effects of the transleaflet quenching should be accounted for (Fig. 5). A recently suggested procedure (Eq. 3) (Ladokhin, 1997) is applied here in the analysis of the previously published data of Bolen and Holloway (1990) on the quenching of tryptophan fluorescence of a synthetic MSP, incorporated in LUV and SUV made of various brominated lipids (Fig. 6).

This peptide was specifically designed to bring tryptophan deep into the bilayer. Regardless of mode of analysis, this is confirmed by stronger quenching with more deeply located quenchers [data of Bolen and Holloway (1990) redrawn in Fig. 6]. To explain the fact that some fluorescence quenching is observed with the shallow quenchers, the authors suggested that tryptophan quenching with brominated phospholipids occurs via a long-range nonradiative energy transfer Förster-like mechanism (Bolen and Holloway, 1990). However, the conditions for such a mechanism are not met, because neither bromine itself nor dibrominated lipids absorb light in the region of tryptophan emission. The quenching is very likely due to a general heavy atom-induced perturbation of spin-orbital coupling (Kasha, 1952) which in the case of aromatic chromophores will lead to intermolecular singlet-triplet energy transfer or/and induced intramolecular intersystem crossing (Berlman, 1973). In other words, this is a collisional quenching. Therefore, the broadening of the quenching profile of this peptide, as in any other case, is due to the general phenomenon of thermal disorder of both probe and quencher, and to their finite size (Ladokhin, 1997).

As the results presented here have demonstrated, the uncoupling of area and width of the depth-dependent fluorescence quenching profile in either DA or PM will 1) minimize systematic errors in the determination of the depth of membrane penetration of the probe, and 2) provide additional information on transverse heterogeneity and lipid exposure of the probe. Certainly the test of utility of the two methods will require new experiments on systems well-characterized by independent nonfluorescent approaches. Nevertheless, as indicated by examples of OmpA and MSP, the distribution analysis technique is well suited to evaluate membrane penetration of peptides and proteins.

I am very grateful to Drs. P. W. Holloway and S. H. White for helpful discussions and to M. A. Myers for reading the manuscript. My special thanks to Dr. W. C. Wimley for numerous discussions and valuable suggestions, and for reading the manuscript.

This research was supported by grants GM-46823 (to Prof. S. H. White, PI) and AI-22931 (to Prof. M. E. Selsted, PI) from the National Institutes of Health.

REFERENCES

Abrams, F. S., and E. London. 1992. Calibration of the parallax fluorescence quenching method for determination of membrane penetration depth: refinement and comparison of quenching by spin-labeled and brominated lipids. *Biochemistry*. 31:5312–5327.

Abrams, F. S., and E. London. 1993. Extension of the parallax analysis of membrane penetration depth to the polar region of model membranes: use of fluorescence quenching by a spin-label attached to the phospholipid polar headgroup. *Biochemistry*. 32:10826–10831.

Asuncion-Punzalan, E., and E. London. 1995. Control of the depth of molecules within membranes by polar groups: determination of the location of anthracene-labeled probes in model membranes by parallax analysis of nitroxide-labeled phospholipid induced fluorescence quenching. *Biochemistry*. 34:11460–11466.

Berkhout, T. A., A. Rietveld, and B. de Kruijff. 1987. Preferential lipid association and mode of penetration of apocytochrome *c* in mixed model membranes as monitored by tryptophanyl fluorescence quenching using brominated phospholipids. *Biochim. Biophys. Acta*. 897:1–4.

Berlman, I. B. 1973. Empirical study of heavy-atom collisional quenching of the fluorescence state of aromatic compounds in solution. *J. Phys. Chem.* 77:562–567.

Bolen, E. J., and P. W. Holloway. 1990. Quenching of tryptophan fluorescence by brominated phospholipid. *Biochemistry*. 29:9638–9643.

Castanho, M., and M. Prieto. 1995. Filipin fluorescence quenching by spin-labeled probes: studies in aqueous solution and in a membrane model system. *Biophys. J.* 69:155–168.

Chattopadhyay, A., and E. London. 1987. Parallax method for direct measurement of membrane penetration depth utilizing fluorescence quenching by spin-labeled phospholipids. *Biochemistry*. 26:39–45.

Chung, L. A., J. D. Lear, and W. F. DeGrado. 1992. Fluorescence studies of the secondary structure and orientation of a model ion channel peptide in phospholipid vesicles. *Biochemistry*. 31:6608–6616.

Clague, M. J., J. R. Knutson, R. Blumenthal, and A. Herrmann. 1991. Interaction of influenza hemagglutinin amino-terminal peptide with phospholipid vesicles: a fluorescence study. *Biochemistry*. 30: 5491–5497.

Everett, J., A. Zlotnick, J. Tennyson, and P. W. Holloway. 1986. Fluorescence quenching of cytochrome b5 in vesicles with an asymmetric transbilayer distribution of brominated phosphatidylcholine. *J. Biol. Chem.* 261:6725–6729.

González-Mañas, J. M., J. H. Lakey, and F. Pattus. 1992. Brominated phospholipids as a tool for monitoring the membrane insertion of colicin A. *Biochemistry*. 31:7294–7300.

Green, S. A., D. J. Simpson, G. Zhou, P. S. Ho, and N. V. Blough. 1990. Intramolecular quenching of excited singlet states by stable nitroxyl radicals. *J. Am. Chem. Soc.* 112:7337–7346.

Hubbell, W. L., and C. Altenbach. 1994. Investigation of structure and dynamics in membrane proteins using site-directed spin labeling. *Curr. Opin. Struct. Biol.* 4:566–573.

Jones, J. D., and L. M. Gierasch. 1994. Effect of charged residue substitutions on the membrane-interactive properties of signal sequences of the *Escherichia coli* LamB protein. *Biophys. J.* 67:1534–1545.

Kachel, K., E. Asuncion-Punzalan, and E. London. 1995. Anchoring of tryptophan and tyrosine analogs at the hydrocarbon-polar boundary in model membrane vesicles: parallax analysis of fluorescence quenching induced by nitroxide-labeled phospholipids. *Biochemistry*. 34: 15475–15479.

Kasha, M. 1952. Collisional perturbation of spin-orbital coupling and the mechanism of fluorescence quenching. A visual demonstration of the perturbation. *J. Chem. Phys.* 20:71–74.

Kleinschmidt, J. H., and L. K. Tamm. 1998. Time-resolved Trp-fluorescence quenching (TIRFQ): probing intermediates during membrane protein folding. *Biophys. J.* 74:15*a*. (Abstr.).

Ladokhin, A. S. 1993. Distribution analysis of membrane penetration by depth dependent fluorescence quenching. *Biophys. J.* 64:290*a*. (Abstr.).

Ladokhin, A. S. 1997. Distribution analysis of depth-dependent fluorescence quenching in membranes: a practical guide. *Methods Enzymol.* 278:462–473.

Ladokhin, A. S., and P. W. Holloway. 1995a. Fluorescence of membrane-bound tryptophan octyl ester: a model for studying intrinsic fluorescence of protein-membrane interactions. *Biophys. J.* 69:506–517.

Ladokhin, A. S., and P. W. Holloway. 1995b. Fluorescence quenching study of melittin-membrane interactions. *Ukrainian Biochemical Journal*. 67:34–40.

Ladokhin, A. S., P. W. Holloway, and E. G. Kostrzhevska. 1993a. Distribution analysis of membrane penetration of proteins by depth-dependent fluorescence quenching. *J. Fluorescence*. 3:195–197.

Ladokhin, A. S., L. Wang, A. W. Steggles, H. Malak, and P. W. Holloway. 1993b. Fluorescence study of a temperature-induced conversion from the "loose" to the "tight" binding form of membrane-bound cytochrome b_5. *Biochemistry*. 32:6951–6956.

Lewis, B. A., and D. M. Engelman. 1983. Lipid bilayer thickness varies linearly with acyl chain length in fluid phosphatidylcholine vesicles. *J. Mol. Biol.* 166:211–217.

Liu, L.-P., and C. M. Deber. 1997. Anionic phospholipids modulate peptide insertion into membranes. *Biochemistry*. 36:5476–5482.

Macêdo, Z. S., T. A. Furquim, and A. S. Ito. 1996. Estimation of average depth of penetration of melanotropins in dimyristoylphosphatidylglycerol vesicles. *Biophys. Chem.* 59:193–202.

Matko, J., K. Ohki, and M. Edidin. 1992. Luminescence quenching by nitroxide spin labels in aqueous solution: studies on the mechanism of quenching. *Biochemistry*. 31:703–711.

Matsuzaki, K., O. Murase, H. Tokuda, S. Funakoshi, N. Fujii, and K. Miyajima. 1994. Orientational and aggregational states of magainin 2 in phospholipid bilayers. *Biochemistry*. 33:3342–3349.

McIntosh, T. J., and P. W. Holloway. 1987. Determination of the depth of bromine atoms in bilayers formed from bromolipid probes. *Biochemistry*. 26:1783–1788.

Meers, P. 1990. Location of tryptophans in membrane-bound annexins. *Biochemistry*. 29:3325–3330.

Mishra, V. K., and M. N. Palgunachari. 1996. Interaction of model class A_1, class A_2, and class Y amphipathic helical peptides with membranes. *Biochemistry*. 35:11210–11220.

Oren, Z., and Y. Shai. 1997. Selective lysis of bacteria but not mammalian cells by diastereomers of melittin: structure-function study. *Biochemistry*. 36:1826–1835.

Pastor, R. W., R. M. Venable, and M. Karplus. 1991. Model for the structure of the lipid bilayer. *Proc. Natl. Acad. Sci. USA*. 88:892–896.

Piknová, B., D. Marsh, and T. E. Thompson. 1996. Fluorescence quenching study of percolation and compartmentalization in two-phase lipid bilayers. *Biophys. J.* 71:892–897.

Rodionova, N. A., S. A. Tatulian, T. Surrey, F. Jähnig, and L. K. Tamm. 1995. Characterization of two membrane-bound forms of OmpA. *Biochemistry*. 34:1921–1929.

Sassaroli, M., M. Ruonala, J. Virtanen, M. Vauhkonen, and P. Somerharju. 1995. Transversal distribution of acyl-linked pyrene moieties in liquid-crystalline phosphatidylcholine bilayers. A fluorescence quenching study. *Biochemistry*. 34:8843–8851.

Silvius, J. R. 1992. Cholesterol modulation of lipid intermixing in phospholipid and glycosphingolipid mixtures. Evaluation using fluorescent lipid probes and brominated lipid quenchers. *Biochemistry*. 31: 3398–3408.

Voges, K.-P., G. Jung, and W. H. Sawyer. 1987. Depth-dependent fluorescent quenching of a tryptophan residue located at defined positions on a rigid 21-peptide helix in liposomes. *Biochim. Biophys. Acta*. 896: 64–76.

White, S. H., and M. C. Wiener. 1995. Determination of the structure of fluid lipid bilayer membranes. *In* Permeability and Stability of Lipid Bilayers. E. A. Disalvo and S. A. Simon, editors. CRC Press, Boca Raton. 1–19.

White, S. H., and W. C. Wimley. 1994. Peptides in lipid bilayers: structural and thermodynamic basis for partitioning and folding. *Curr. Opin. Struct. Biol.* 4:79–86.

Wiener, M. C., and S. H. White. 1991. Transbilayer distribution of bromine in fluid bilayers containing a specifically brominated analog of dioleoylphosphatidylcholine. *Biochemistry*. 30:6997–7008.

Yeager, M. D., and G. W. Feigenson. 1990. Fluorescence quenching in model membranes: phospholipid acyl chain distributions around small fluorophores. *Biochemistry*. 29:4380–4392.